HOSTED BY
ELSEVIER
Available online at www.sciencedirect.com
ScienceDirect
Soils and Foundations 62 (2022) 101091
www.elsevier.com/locate/sandf

Technical Paper

Evaluation of the damping ratio of soils in a resonant column using different methods

Kunjari Mog, P. Anbazhagan *

Department of Civil Engineering, Indian Institute of Science, Bangalore 560012, India

Received 26 August 2020; received in revised form 21 October 2021; accepted 8 November 2021
Available online 13 December 2021

Abstract

This paper addresses the differences between two approaches of damping estimation in the resonant column testing: Steady-State Vibration (SSV) and Free Vibration Decay (FVD) method, at small (<0.005%) to medium (0.07%) strain range. The tests were conducted on "two types of reconstituted sands" and "two types of clayey soils" at different relative densities and confining pressures. The test results suggested to use the SSV method in small strain damping measurement and the FVD method (two or three successive cycles) in medium strain damping measurement. A systematic decrease in the damping with the increasing number of cycles was observed up to a certain strain level in the FVD method. Furthermore, the effects of relative density, confining pressures, soil types on the damping ratio derived from the two methods for the chosen soils were studied. The results showed that the damping ratio of clayey soils exhibits a little higher value than those of sandy soils.

Keywords: Resonant column; Damping ratio; Free-vibration decay; Steady-state vibration; Small to medium shear strain; Sands; Silty-sands; Clayey soils

1. Introduction

The damping ratio is commonly used to measure the energy dissipation of a vibrating body due to the dynamic or cyclic loading. The response of the super-structures under dynamic loading conditions depends on the local soil properties that exist underneath. Small strain stiffness and damping properties help establish realistic predictions of the ground movement of the underlying infrastructures due to vibrations. Most often, the dynamic response of the structure is effectively controlled by changing the damping in the system. Hence, the estimation of damping at near-resonance frequencies became vital in the dynamic analysis of a soil mass to predict realistic behavior. Several studies have revealed that the shear strain amplitude, effective confining pressure, number of loading cycles are the major contributing factors influencing the damping ratio of soils; the sand type has a moderate effect; and the relative density, plasticity index, over-consolidation ratio, frequency of loading cycles, moisture content and method of sample preparation has a little effect (Hardin and Drnevich, 1972; Kokusho, 1980; Ni, 1987; Vucetic and Dobry, 1991; Darendeli, 2001; Zhang et al., 2005; Kokusho et al., 2005; Sitharam et al., 2008; Senetakis et al., 2012; Senetakis and Madhusudhan, 2015; Mog and Anbazhagan, 2018). Nevertheless, the energy dissipation phenomenon at a small strain level is not fully understood in the literature (Payan et al., 2016). The small strain damping ratio also shows a strong dependency on the particle shape parameter such as roundness and sphericity (Santamarina and Cascante,1998; Cho et al., 2007; Senetakis et al., 2012; Payan et al., 2016).

A significant development in the laboratory measurement of soil damping happened in the soil dynamics field

Peer review under responsibility of The Japanese Geotechnical Society.
* Corresponding author.
E-mail address: anbazhagan@iisc.ac.in (P. Anbazhagan).

https://doi.org/10.1016/j.sandf.2021.101091

in the 1960s and 1970s (Hardin and Drnevich, 1972). Nevertheless, much attention is still needed to accurately model the realistic damping behavior of soil and understand the fundamentals of the energy dissipation phenomenon at small strains. Although in-situ testing techniques are promising, it is difficult to directly measure the dynamic soil properties in the field at medium to large strain ranges (Yamamizu et al., 1983; Kokusho et al., 2005). Thus, it seems that laboratory testing would continue to be essential to understand the dynamic soil behavior under cyclic or irregular earthquake loading conditions.

In resonant column testing, damping is determined either from the Steady-State Vibration (SSV) or Free Vibration Decay (FVD) method. The SSV is also known as half-power bandwidth and FVD as logarithmic decrement method. In the first method, the soil specimen is vibrated at its first mode of natural frequency, in which the steady-state peak amplitude at resonance is used to obtain the damping ratio. In the second method, after removing the forced vibration, the specimen is allowed to vibrate freely; simultaneously, the amplitude of the decaying motion with time is recorded, and the damping ratio is calculated accordingly. Prior studies (Papagiannopoulos and Hatzigeorgiou, 2011; Wang et al., 2012) have suggested a third-order correction to the half-power bandwidth method to accurately estimate the damping of the single degree of freedom and multi-degree of freedom systems. Though, the comparisons between the SSV and FVD methods of damping estimation in the resonant column testing are limited in the literature.

In the previous work, Senetakis et al. (2015) recommended using two successive cycles of damping ratio; and Stokoe et al. (1999) suggested using three successive cycles for damping determination in FVD. The ASTM (D4015-1992) specification suggested that the number of cycles no more than ten should be used to determine the damping ratio from the free vibrations data. However, the preferable method concerning the shear strain range is not specified clearly. Hence, the purpose of this study is to detail investigate the differences between the SSV and FVD methods for the determination of damping in a resonant column testing and suggest the appropriate method to be adopted depending on the working shear strain range. Besides, the damping results of natural sands and clayey soils obtained from the SSV and FVD methods corresponding to the suggested shear strain range are adopted and discussed in the paper.

1.1. Test materials and sample preparation

The four different soil materials obtained from different locations in India were tested in resonant column equipment. The soils were identified as clean sand, silty sand, and two clayey soils, designated as samples A, B, C, and D in this study. The damping ratio of these soils was investigated using SSV and FVD methods in the small to medium strain levels. The information regarding the index properties, maximum and minimum dry density, USCS (Unified Soil Classification System) (ASTM, 2017; ASTM, 2000) classification are given in Table 1. The grain size distribution curves of four soils, including the plasticity index chart of "two types of clayey soils," are shown in Fig. 1. All the soil samples were obtained by auger boring and pit excavation of depths ranging from 1 m to 5 m approximately. Based on the USCS classification, these soils fall under the category of (1) sample A – poorly graded sand (SP), (2) sample B – silty sand (SM), (3) sample C – clay of low plasticity (CL), (4) sample D – clay of low plasticity (CL). Samples C and D may be referred to as clayey silt as both samples contained about 70% of silt (with clay contents of 21% and 10% in the mixture) (see Table 1).

The Scanning Electronic Microscope (SEM) images of the four tested materials captured at different magnifications are provided in the supplementary file as an appendix in Fig. A1. The SEM imaged particles of the sandy materials (sample A and sample B) were analyzed digitally using the image analysis software called ImageJ and particle shape descriptor such as roundness and circularity (sphericity in 3-dimension) parameters were quantified. For a givens sand, 80 particles were randomly selected to characterize the shape of the granular sand, and only the mean values were considered. Sample A is clean sand, whereas sample B contains about 20% silt (Table 1). The roundness and circularity values of sample A are 0.692, 0.738, and sample B is 0.679, 0.621, respectively. Both samples A and B fall in approximately the same roundness category (subrounded to the rounded group). However, the circularity characteristic of sample A is greater than that of sample B.

The dry-tamping method is adopted to prepare all the tests specimen of size 50.4 mm in diameter and 102 mm in height. The samples were tested at three different relative densities viz. 30%, 60%, and 80% under the confining pressures of 50, 100, 200 kPa. The details of the sample preparation of dry soil were described in Mog and Anbazhagan (2018). The summary of the tests performed under the resonant column equipment is given in Table 2.

1.2. Measurement of damping in resonant column apparatus

The resonant column is the most commonly used laboratory test to measure the soil damping at small to medium strains. In the present study, the Geotechnical Consulting and Test Systems (GCTS) fixed-free resonant column apparatus is used in which a cylindrical soil specimen is restrained at the base, and cyclic torsional load is applied at the top. The external excitation at the top of the soil column is given by an electromagnetic drive system or motor attached to it. The top of the specimen is constrained in the horizontal direction to prevent any bending of the soil column during testing. In this, first, a torsional harmonic load is applied, and the loading frequency of the input vibration is gradually varied until the resonant frequency is found

Table 1
Basic properties of the test samples used in the present study.

Characteristics	Unit	Sample A	Sample B	Sample C	Sample D
Specific gravity	–	2.67	2.63	2.73	2.59
Liquid limit	%	–	–	30	30
Plastic limit	%	–	–	18	21
Plasticity index	–	Non-plastic	Non-plastic	12	9
Gravel content	%	0.846	–	–	–
Sand content	%	98.95	79.75	12.09	18.67
Silt content	%	0.196	19.83	66.91	71.33
Clay content	%	–	0.410	21	10
Maximum dry unit weight	g/cc	1.855	1.741	1.730	1.177
Minimum dry unit weight	g/cc	1.596	1.395	1.179	1.675
USCS classification	–	SP (Poorly graded sand	SM (Silty sand)	CL (Clay of low plasticity)	CL (Clay of low plasticity)

(Maximum response or maximum strain amplitude). The frequency at which the maximum response is encountered is the resonant frequency of the soil specimen. The shear wave velocity is then calculated from the first mode of resonance frequency, which in turn provides the shear modulus. The shear wave velocity is calculated from the governing equation of motion for the fixed-free resonant column system:

$$\frac{I}{I_0} = \frac{\omega h}{V_s}\tan\left(\frac{\omega h}{V_s}\right) \tag{1}$$

where

I = mass moment of inertia of the soil column equals $\frac{md^2}{8}$
m = total soil mass
d = diameter of the soil column
I_0 = mass moment of inertia of the drive system including the top cap or added mass
V_s = shear wave velocity of the soil column
ω = natural circular frequency of the soil column
h = height of the specimen

The values of I and h can be easily determined from the specimen dimension and weight. I_0 can be regarded as a system constant which is determined from the calibration of the drive plate, described in section 3.3. In the resonant column test, the resonant frequency is measured instead of the natural frequency of the specimen. Hence, the resonant frequency is used to calculate the V_s assuming that the resonant frequency and natural frequency are equal when the damping ratio is small. This assumption seems valid for small strain damping measurements of most soils where the damping ratio is <12% (Ni, 1987).

Once the shear wave velocity, V_s is determined using Eq. (1), the dynamic shear modulus, G is calculated from the relationship:

$$G = \rho {V_s}^2 \tag{2}$$

where ρ is soil mass density.

The material damping can be determined either from the width of the frequency response curve or the free vibration decay curve in the resonant column test, which is discussed in the following section. In all cases, the equipment-generated damping or apparatus damping was accounted for while making damping measurements.

1.3. Determination of damping ratio from free vibration decay method

It is difficult to define the true material damping as damping mechanism (internal damping) of soil materials is not yet well understood. However, in usual practice, the soil damping is interpreted in terms of its equivalent viscous damping ratio. The term damping ratio is applied only to the single degree of freedom systems, and the most common form of damping expression used in geotechnical engineering application is as follows (Ishihara, 1996):

$$D = \frac{C}{C_c} \tag{3}$$

where, D is viscous damping ratio or fraction of critical damping, C is the coefficient of damping, andC_c is critical damping. Again, the critical damping C_c is related to the stiffness, k, and mass, m, as follows:

$$C_c = 2\sqrt{km} \tag{4}$$

In the resonant column test, after the steady-state vibration is removed or when the power of the electromagnetic drive system is shut off, free vibration decay takes place, in which mode soil specimen can vibrate freely under the action of forces inherent in the system itself. The amplitude of the decaying motion is recorded using the accelerometer mounted on the resonant column drive system. The damping is then determined from the measurement of the logarithmic decrement (δ), which is defined as the natural logarithm of the ratio of the amplitudes at subsequent cycles.

$$\delta = ln\frac{x_n}{x_{n+1}} \tag{5}$$

where, x_n is peak displacement of the n-th cycle, $x_{n+1}$is peak displacement of the next $(n + 1)$ cycle.

In this case, once logarithmic decrement (δ) is measured, material damping is calculated from the following equation:

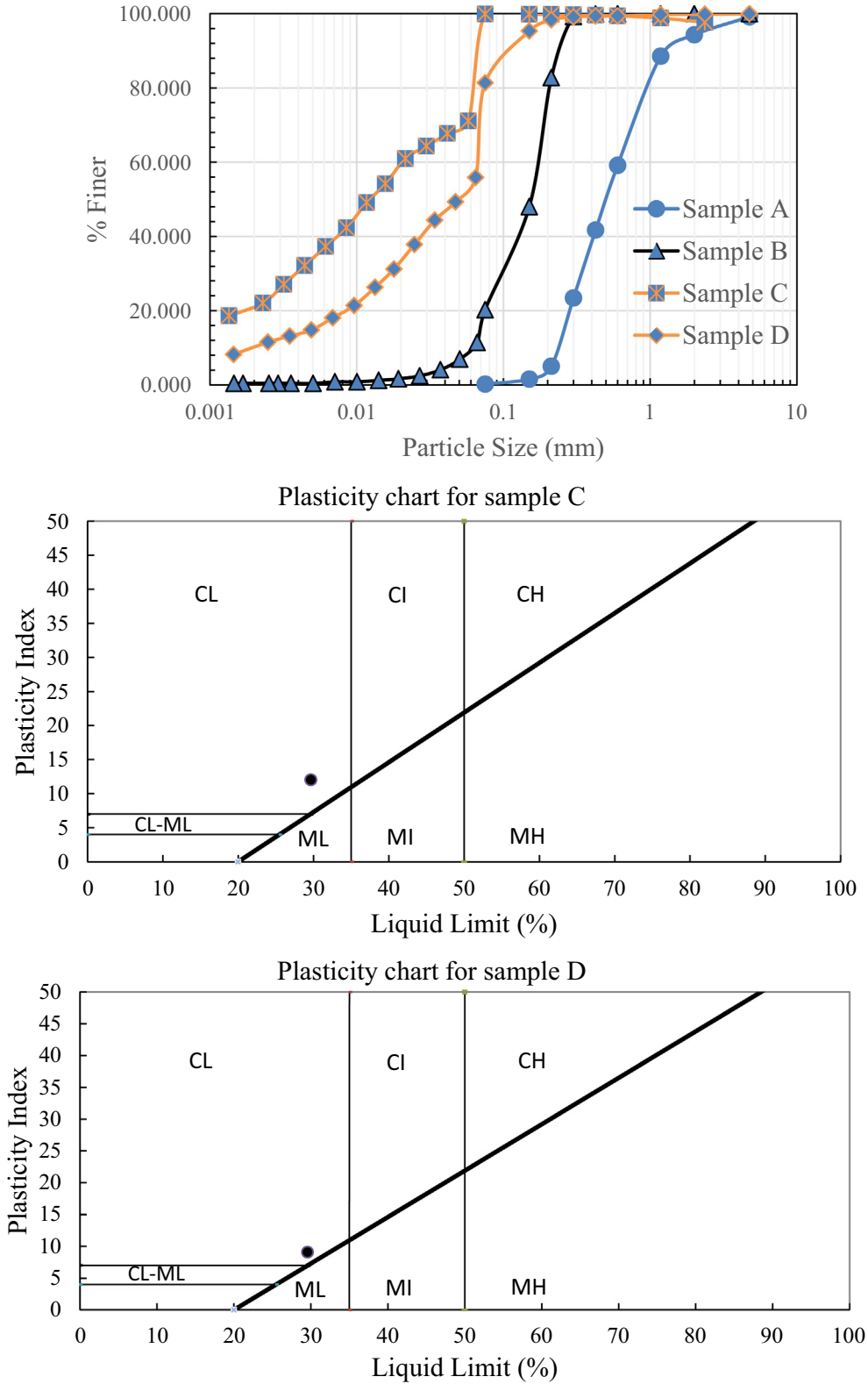

Fig. 1. Grain size distribution and plasticity index of the tested soi materials.

$$D = \sqrt{\frac{\delta^2}{4\pi^2 + \delta^2}} \tag{6}$$

The Free Vibration Decay (FVD) damping ratio is calculated using Eq. (6). The GCTS resonant column software records the free vibration data for all the cycles with a shear strain amplitude of at least 15% of the maximum shear strain obtained during the forced vibration test (or SSV). The typical free vibration decay curve of a soil sample obtained during the resonant column testing is

Table 2
Summary of the test programs conducted in the present study.

Test number	Test material	Relative density (%)	Confining pressures (kPa)	Torque applied (pfs)
1	Sample A	30	50	0.05, 0.1, 0.5, 1.0, 2.0, 3.0, 5.0, 8.0, 10.0, 15.0, 20.0, 30.0, 40.0
2	Sample A	30	100	
3	Sample A	30	200	
4	Sample A	60	50	
5	Sample A	60	100	
6	Sample A	60	200	
7	Sample A	80	50	
8	Sample A	80	100	
9	Sample A	80	200	
10	Sample B	30	50	0.05, 0.1, 0.5, 1.0, 2.0, 3.0, 5.0, 8.0, 10.0, 15.0
11	Sample B	30	100	
12	Sample B	30	200	
13	Sample B	60	200	
14	Sample B	80	50	
15	Sample B	80	100	
16	Sample B	80	200	
17	Sample C	60	50	0.05, 0.1, 0.5, 1.0, 2.0, 3.0, 5.0, 8.0, 10.0
18	Sample C	60	100	
19	Sample C	60	200	
20	Sample C	80	50	
21	Sample C	80	100	
22	Sample C	80	200	
23	Sample D	30	50	0.05, 0.1, 0.5, 1.0, 2.0, 3.0, 5.0, 8.0, 10.0, 15.0, 20.0, 25.0
24	Sample D	30	100	
25	Sample D	30	200	
26	Sample D	60	50	
27	Sample D	60	100	
28	Sample D	60	200	
29	Sample D	80	100	
30	Sample D	80	200	

presented in Fig. 2 (right panel). The free vibration decay damping ratio is determined from the slope of the peak shear strain amplitude versus the number of cycles plot obtained from the free vibrations data shown in Fig. 3. A least square analysis is used to calculate the damping ratio and fitted correlation coefficient. The damping ratio is determined for the prescribed number of cycles based on the goodness of the fit (i.e., correlation coefficient value) for the selected peak and valley sensitivity data. The detailed procedure for determining the damping ratio for prescribed cycles from the FVD data of a resonant column test is explained in the appendix (section 1).

In the FVD method, as shown in Fig. 2 (right panel) and Fig. 3, the amplitude of vibrations varies from large to small as the number of cycles increases. In such a case, which shear strain amplitude should be suitable for the damping ratio calculation by Eq. (6) is unclear. Few studies have reported using the average of first two cycles by

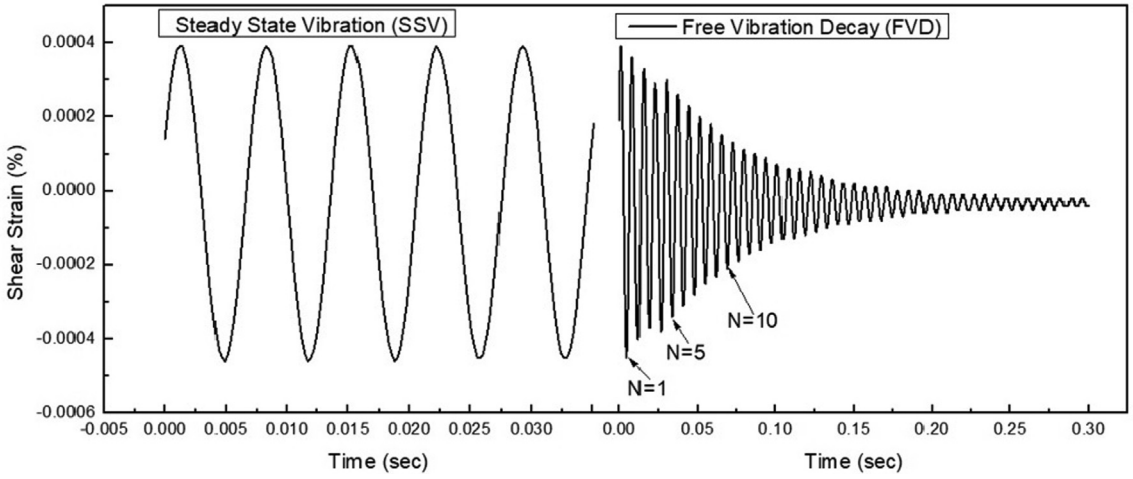

Fig. 2. Typical steady state vibration & free vibration decay curve of soil obtained from resonant column testing.

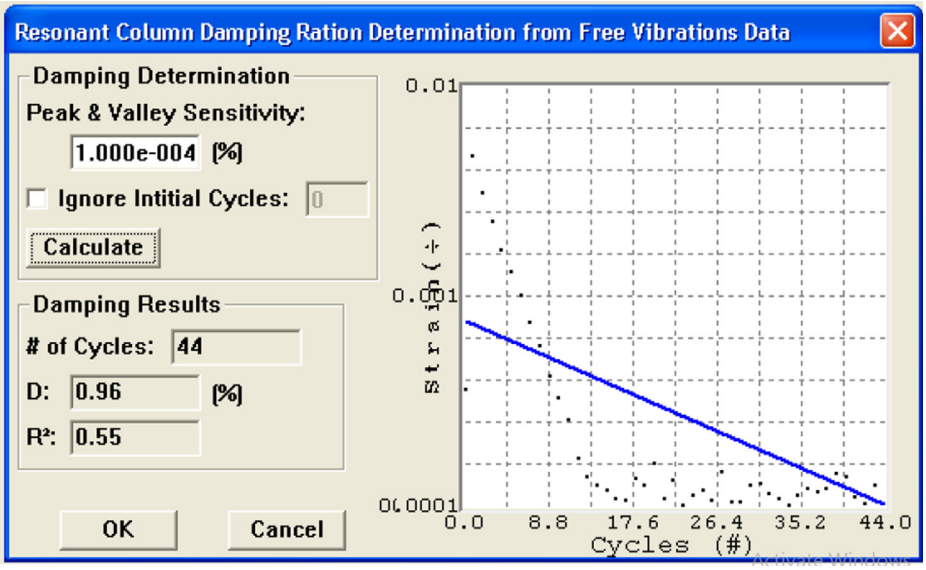

Fig. 3. Strain amplitude versus number of cycles in FVD method.

Senetakis et al. (2015); three cycles by Stokoe et al. (1999); last five powered cycles by Bolton and Wilson (1990); less than ten cycles by ASTM (1992). In contrast, it was stated in the GDS RCA manual (2015) that the fit between 10 and 50 cycles is commonly used in the damping ratio calculation. Thus, it is necessary to evaluate the representative strain (or cycles) for damping ratio calculation when FVD is applied. This aspect has been addressed in the results section.

1.4. Determination of damping ratio from steady state vibration

The Steady-State Vibration (SSV) is also known as the half-power bandwidth method. It is the second method that is popularly used to measure the material damping ratio in the resonant column test. Apart from its application on resonant column tests in soil dynamics, the theory of SSV to harmonic excitation has several applications. These include forced vibration tests on structures, vibration isolations, accelerograph design, etc. In this, the logarithmic decrement (δ), is calculated from the forced vibration test by measuring the width of the frequency response curve near the resonance. The following expression is used to calculate δ (GCTS-CATS, 2007):

$$\delta = \frac{\pi(f_2^2 - f_1^2)}{2f_r^2}\sqrt{\frac{P^2}{P_{max}^2 - P^2}}\frac{\sqrt{1-2D^2}}{1-D^2} \tag{7}$$

where, $f_1$and f_2 are the frequencies below and above the resonance where the strain amplitude is P, P_{max} is the maximum amplitude (or resonant amplitude), f_r is the resonant frequency, and D is the damping ratio of the material. P is also referred to as the half-power points.

When the damping is small and the amplitude$P$ is $\frac{P_{max}}{\sqrt{2}}$, Eq. (7) can be simplified as:

$$\delta \cong \frac{\pi(f_2 - f_1)}{f_r} \tag{8}$$

Then, the damping ratio can be expressed as:

$$D \cong \frac{(f_2 - f_1)}{2f_r} \tag{9}$$

The typical steady-state vibration (left panel) of a soil sample obtained during the resonant column testing is presented in Fig. 2. Fig. 4 represents a typical frequency response curve in the form of strain amplitude versus forcing frequency obtained in the resonant column test. In Fig. 4 (left panel), it can be observed that the half-power bandwidth method consists of measuring the two frequencies f_2 and f_1, where steady-state energy is half of that at the resonant frequency (f_r). The half-power points correspond to the frequencies at which, $P = \frac{P_{max}}{\sqrt{2}}$, where P_{max} is the maximum amplitude as shown in the frequency response curve. The sharpness or width of the frequency response curve near the resonance frequency depends on the presence of damping in the system. Eq. (9) is used to determine the damping in the present study from SSV. The frequency response curves obtained for one of the sand specimens at different applied torque during the resonant column testing are illustrated in Fig. 4 (right panel). In SSV, during the resonance just before turning off for the free-vibration decay test, a soil sample undergoes a numerous number of loading cycles; however, due to the nature of the resonant column test, no data savings is done for those many numbers of cycles, as the data is saved only for the last five cycles. Thus, changes in the specimen's stiffness and damping ratio over the first few hundred of loading cycles cannot be measured in SSV. For a constant sinusoidal torque amplitude in SSV (using the GCTS resonant column system) at a sequence of increasing frequen-

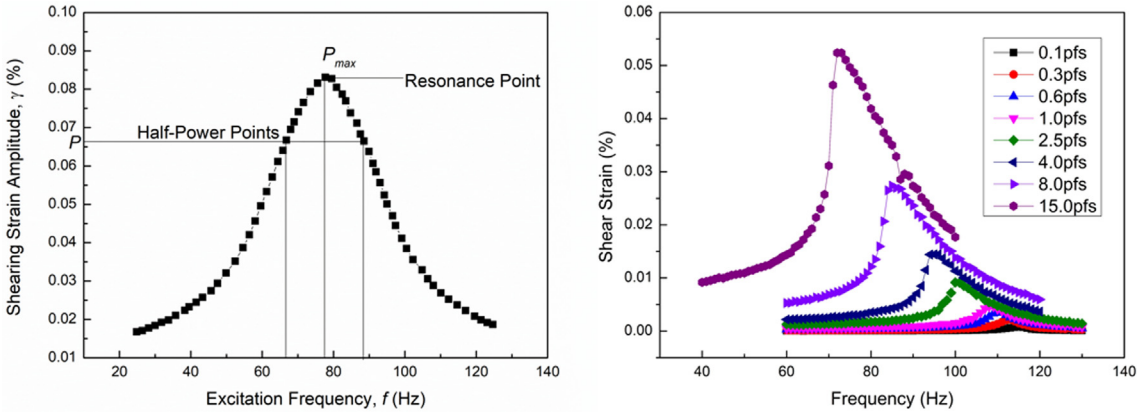

Fig. 4. Typical frequency response curve in the half-power bandwidth method (left Panel). Typical frequency response curves of sand specimen (for sample A) at different torque amplitude (right panel).

cies (frequency sweep) in 1 Hz increment, the total number of cycles applied to a specimen, in each case, ranges between 500 and 1000 cycles in this study.

1.5. Damping of resonant column drive system

The damping results obtained from the resonant column testing are generally the combination of the specimen damping and equipment-generated damping. If equipment damping or apparatus damping is not accounted for in the calculation, it may result in inaccurate values. The apparatus damping can be evaluated from the calibration procedure of the GCTS resonant column drive system. The drive system consists of a driving plate (torsional motor) and a specimen top cap. The damping ratio of resonant column drive system is the inherent damping of resonant column drive system. Thus, all of the calculated specimen damping ratios will have this damping ratio of the drive system subtracted from their value for all the tested soils samples. Prior studies (Papagiannopoulos and Hatzigeorgiou, 2011; Wang et al., 2012; Drnevich and Ashlock, 2017) have also noted the importance of considering the apparatus damping at low strains.

The calibration of the GCTS resonant column drive system is performed using a metallic specimen instead of an actual soil specimen. It is assumed that the metallic specimen (or calibration specimen) should have zero or close to zero dampings with a constant torsional stiffness, k. Then, from Newton's second law, the mass moment of inertia is related to the natural or resonant frequency, ω, as follows:

$$I = \frac{k}{\omega^2} \tag{10}$$

The recommended way to find the mass moment of inertia of the drive system,I_0, is to perform the two resonant column tests on the calibration specimen, first by itself without the added mass and second with added mass. Then perform a frequency sweep operation with constant force amplitude to find the resonant frequency for each configuration. The calibration specimen is made of 6061-T6 aluminum with a mass density of 2.7 g/cm^3. The added mass is made of 303 stainless steel with a mass density of 7.7 g/cm^3. The calibration specimen and added mass geometry are shown in Fig. A2 in the appendix.

The solution to Eq. (10) for the first calibration run without the added mass becomes:

$$I_0 + I_{cal} = \frac{k}{\omega_1^2} \tag{11}$$

The second equation for the second calibration run attaching the added mass becomes:

$$I_0 + I_{cal} + I_{mass} = \frac{k}{\omega_2^2} \tag{12}$$

where

I_0 = mass moment of inertia of the drive system and any other fixture that will be used during actual soil testing,
I_{cal} = mass moment of inertia of the calibration specimen,
ω_1 = resonant frequency of calibration specimen without the added mass,
I_{mass} = mass moment of inertia of the added mass,
ω_2 = resonant frequency of the calibration specimen with the added mass.

Now, combining Eq. (11) and Eq. (12) becomes:

$$I_0 = \frac{(I_{cal} + I_{mass})\omega_2^2 - I_{cal}\omega_1^2}{\omega_1^2 - \omega_2^2} \tag{13}$$

The value of I_0 as obtained from Eq. (13) is used to solve the Eq. (1) to determine the shear wave velocity. For the GCTS resonant column system, the specimen top cap is not used during the calibration procedure. Thus, its mass moment of inertia is added to the result of Eq. (13) to calculate the actual I_0 value. The mass moment of inertia of the top cap is calculated separately from its geometry and mass using the appropriate formula. Using the GCTS resonant column equipment, the damping ratio of the resonant column drive system was found to be 0.33% and 1

% for FVD and SSV, respectively. Therefore, in this study, these values were subtracted from the measured damping ratio of all soil specimens.

2. Results and discussions

The laboratory damping results obtained from the resonant column test using two damping determination techniques (SSV and FVD) are investigated and presented herein. Four different types of reconstituted soils (A, B, C, and D) were tested at three different relative densities (30%, 60%, 80%) with an application of three different effective confining pressures (50, 100, 200 kPa). The test results are presented in the form of a plot of the variation of damping ratio with respect to shear strain, with a comparison of both SSV and FVD methods. Particular attention is also made to the changes in the value of damping ratio while a different successive number of cycles (i.e., 2, 3, 10, 20, 30, 50 cycles) is selected in FVD; and the appropriate number of cycles to be adopted for the analysis is highlighted. Furthermore, the influence of the nature of the soil type, relative density, confining pressures on the damping properties is presented and compared with the available data in the literature.

3. Effect of number of successive cycles on damping ratio at small to medium strain levels

As previously discussed, due to the nature of the resonant column test, the study of the effect of the number of loading cycles on the damping ratio using the SSV method is beyond the scope. On the other hand, in the FVD method, the strain amplitude decreases with the number of cycles increases (Fig. 2, right panel and Fig. 3). Hence, it is unclear which strain amplitude should be regarded as a representative strain or which number of oscillations should be considered for calculating the damping ratio. Thus, this aspect has been investigated using a fixed-free resonant column apparatus and calculating the damping ratio at various cycles in FVD. Two types of sandy soil and two types of clayey soils named samples A, B, C, and D were used. The results of the resonant column tests on samples A, C, and D, corresponding to 60% relative density under a confining pressure of 100 kPa and 200 kPa, is presented in Fig. 5(a)–(d). The damping is calculated using Eq. (6) of FVD and Eq. (9) of SSV method, as explained in the preceding section. The damping ratio obtained from FVD for prescribed cycles of 2, 3, 7, 10, 20, 30, and 50 cycles is shown in Fig. 5 and Fig. 6. The

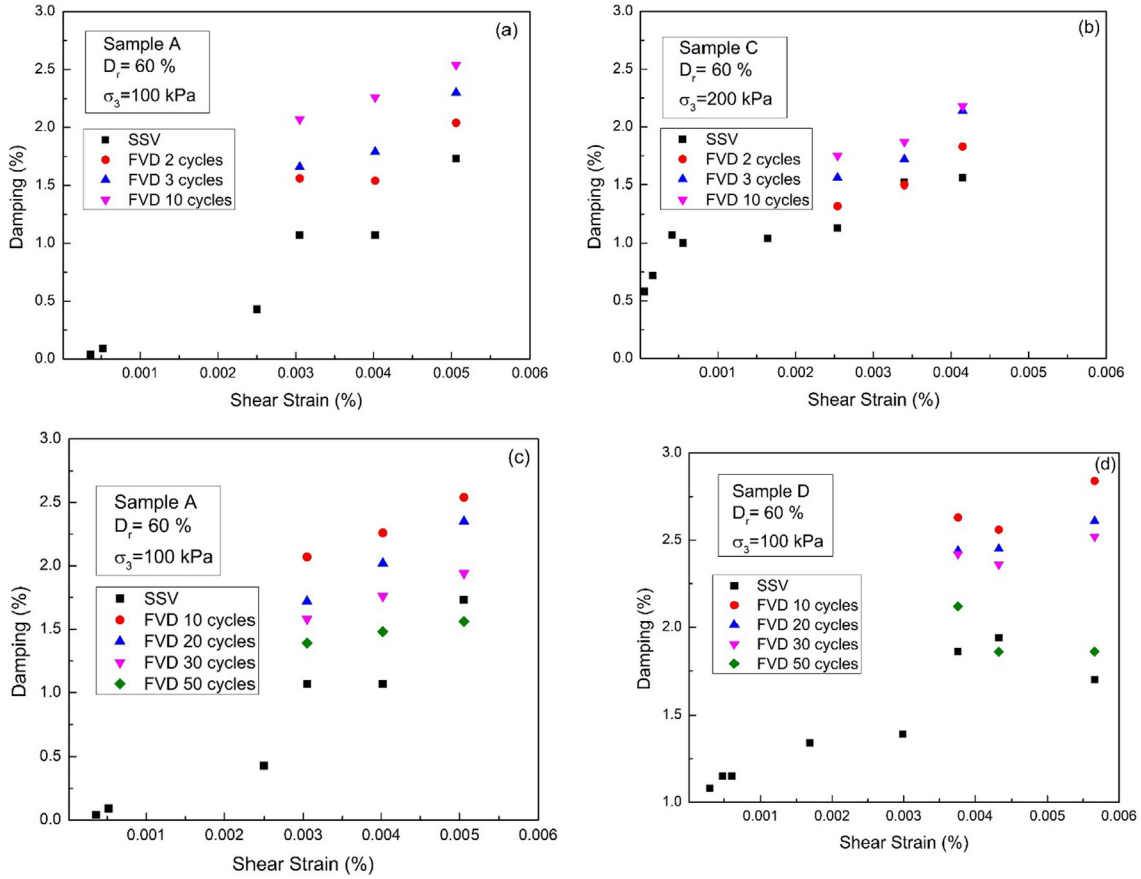

Fig. 5. Damping versus shear strain amplitude using SSV and FVD at small strain levels, (a) and (b) illustrates the results for sample A and sample C, for the prescribed smaller number of cycles at 2, 3, 10 cycles; (c) and (d) shows the results for sample A and sample D, at a higher number of cycles (at 20, 30, 50 cycles).

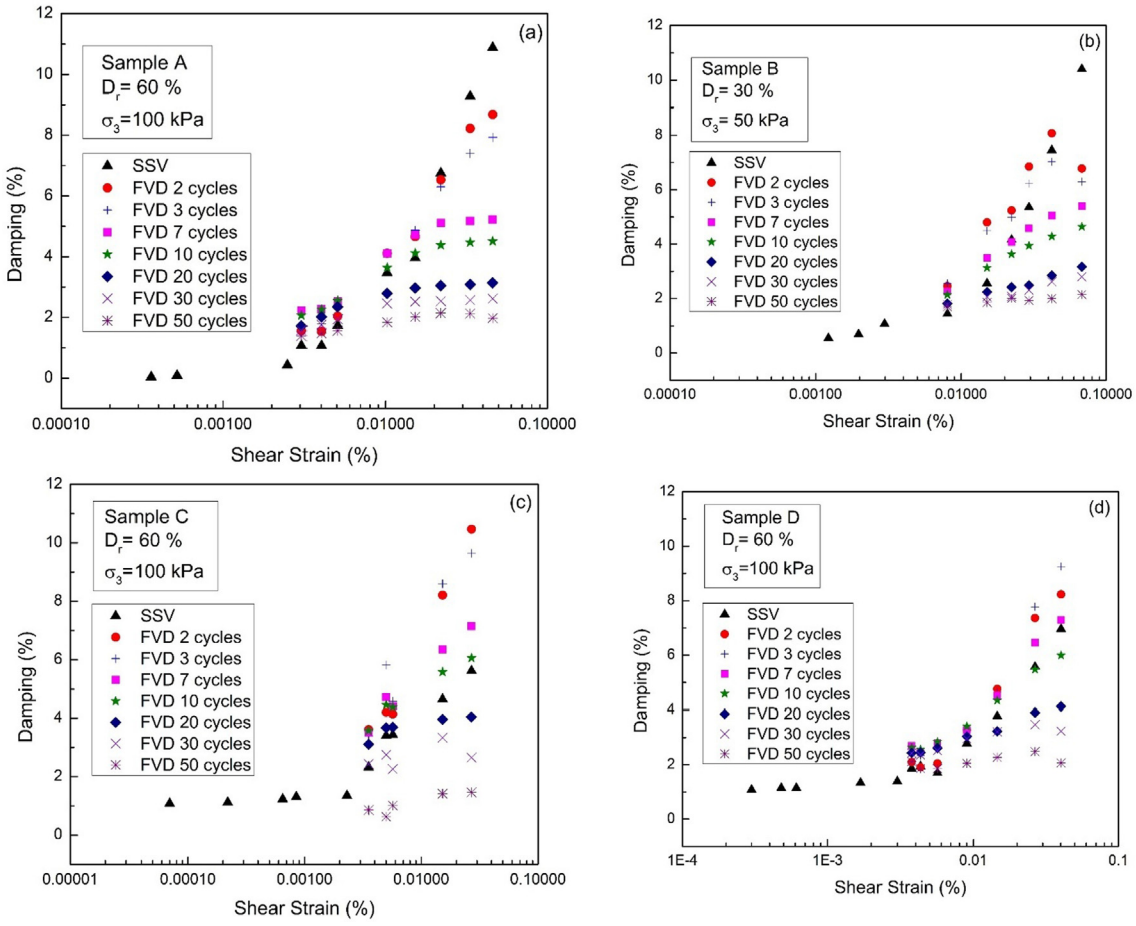

Fig. 6. Variation of damping with shear strain amplitude using SSV and FVD at small to medium strain levels for various number of cycles, (a) for Sample A, (b) for Sample B, (c) for Sample C, and (d) for Sample D.

damping ratio obtained using the SSV method has also been shown in Fig. 5 (square symbol) and Fig. 6 (triangle symbol) for comparison purposes. The variation of damping ratio against the shear strain amplitude for prescribed cycles of 2, 3, 10 (referred to as the smaller number of cycles) are shown in Fig. 5(a) and (b). Similarly, variation of damping ratio against the shear strain for prescribed cycles of 10, 20, 30, 50 (referred to as the higher number of cycles) are shown in Fig. 5(c) and (d).

Data from several studies suggest that there exists a threshold strain for soils subjected to dynamic loading (Hardin and Drnevich, 1972, Ni, 1987). The threshold strain is the strain amplitude below which dynamic soil properties such as stiffness, and material damping are constant or independent of shearing strain amplitude (i.e., soil exhibits linear behaviour). The dynamic properties measured at these strain levels are called the small strain shear moduli and small strain damping ratio. Above the threshold strain, when soil is cycled, it exhibits non-linear behaviour. The exact strain threshold may vary between 0.001% and 0.005% depending on the soil type (sand, clay, or soil with fines) and confining pressure, as shown later in this paper. The strain level below 0.005% is referred to as the small strain damping, and strain level above 0.005% is referred to as the medium strain damping in this study while comparing the test results.

It can be seen from Fig. 5(a) and (b) that an increase in damping is observed with the progression of cycles (up to 10 cycles) and with the increase in shear strain using the FVD method. In Fig. 5(c) and (d), damping values after the application of the 10th cycles are shown where a decreasing trend of damping ratio is noticed with the progressive number of cycles (i.e., for 20, 30, 50 cycles). This systematic trend of increase of damping up to 10 cycles and decrease of damping after 10 cycles is mostly similar irrespective of the soil types chosen in the study. The percentage variation in the damping results of the FVD method is pretty much high in the small strain range for 2 and 10 cycles. It can also be observed that the damping ratio derived from the SSV method is low compared to the FVD method (at the various number of cycles) in small strain levels (<0.005). One reason may be attributed to the contribution of the ambient noise (Meng, 2003) and other potential sources of error present during the resonant column testing on the free vibration decay curve. At small strain and low confining pressure, the electronic signal is small compared to the surrounding background (or ambient noise). Thus, the measured amplitude of vibrations may

randomly get affected by the background noise and affect the calculated damping ratio.

The variation of the damping ratio at small to medium strains, obtained from the same test series for samples A, B, C, and D, are presented in Fig. 6(a)–(d). The selected test results are shown in the form of a plot of damping ratio versus shear strain amplitude for the various number of successive cycles. It can be seen from Fig. 6(a) that the damping ratio obtained at the 2nd and 3rd cycles is close to each other when shear strain amplitude is >0.005%, in the FVD method; and approximately, the same damping value was observed for SSV method. Similar results were also noticed (in strain ranges >0.005 and <0.04%) for other soil samples as well, which can be seen in Fig. 6(b)–(d). Further, the trend of increase in damping ratio with an increase in shear strain amplitude was observed irrespective of chosen soil types at a smaller number of cycles. This increase is certainly attributed to a non-linear increase which is very much pronounced at 10 or fewer cycles. However, this increase of damping ratio with an increase in shear strain amplitude begins to be unnoticeable at 20 successive cycles or higher cycles [Fig. 6(a), (b)]. That is, the changes in damping ratio are nearly constant at a larger number of cycles in the free-vibration decay method. It is because the goodness of the fit deteriorates (due to non-linear fits in the free vibrations data) with the increasing number of cycles or at higher cycles, which can be clearly seen from Fig. 3 (and as explained in appendix section 1). At larger cycles, as the wave amplitude is very small or completely damped after the 20th or 30th cycles (depending on the applied strain amplitudes), the calculated damping ratio is underestimated. If the peak strain amplitude is less than the threshold strain, in that case, the logarithmic decrement, which is the slope of log amplitude versus the number of cycles, is constant from one cycle to the next, i.e., the linear visco-elastic theory is valid. However, if the peak strain is greater than the threshold strain, the linear relationships no longer hold, and thus, the logarithmic decrement is no longer constant. Therefore, scattering in the damping data in FVD at larger number of cycles is inherent due to a change in the logarithmic decrement or slope of the log amplitude versus the number of cycles.

Hence, it can be concluded that there is a considerable effect of the successive number of cycles on the damping ratio in the FVD method. The damping ratio increases with increasing cycles between 2 and 10, followed by the decrease thereafter, as illustrated in Fig. 5. The possible reason for this can be attributed to the slight variation in void ratio due to the rearrangement of the soil particles without any appreciable change in the specimen height and due to the inherent scatter of the damping ratio calculation determined by the free vibration decay curves at small strain amplitude. The ASTM (D4015-1992) specification suggested using ten or fewer number of free vibration cycles (though, depending on the shear strain range, which method should be adopted is not specified clearly). However, it can be seen from Figs. 5 and 6 that there is a significant variation in the damping ratio between 2 and 10 successive cycles over a wide shear strain amplitude. Therefore, using 2 or 3 successive cycles is preferable when FVD is used for determining the damping ratio in the resonant column test at medium strain levels.

4. Comparison of the SSV and FVD

The obtained values of the damping ratio extracted from the SSV and FVD method corresponding to various relative densities and confining pressures are compared and presented in Figs. 7 and 8. Fig. 7 shows a comparison of material damping obtained from the SSV and FVD for soil sample A (SP) at small strain ranges (less than or equal to 0.005%). The damping ratio obtained at the two successive cycles derived from FVD is used to compare with SSV. It can be observed from Fig. 7 that the scatter of the data between the steady-state and free-vibration decay method is found to be more than ±15% at small shear strain levels. Most data points fall on the lower side of the equivalent line (1:1). Likewise, large scattering in the damping data (even >50% difference) is found between the two methods when 3, 7, 10th successive cycles are considered in small shear strain ranges. A significant difference in damping value was also observed for soils B, C, and D samples in small shear strain levels. The difference in the damping ratios between the two methods stems from ambient noise's contribution (as previously discussed) and partly due to the number of applied cycles more than thousands in SSV and only tens in FVD.

The frequency response curve in the half-power bandwidth method is symmetrical at lower strain amplitude, i.e., when applied strain amplitude is smaller than the threshold strain. However, as shown in Fig. 4 (right panel), this symmetry is no longer maintained for strain-level larger than the threshold strain (0.005%). If the strain amplitude is extremely large, the jump phenomenon commonly occurs in the frequency response curves; hence, one half-power point cannot be precisely located. This causes a serious error in the damping calculation. Thus, the half-power

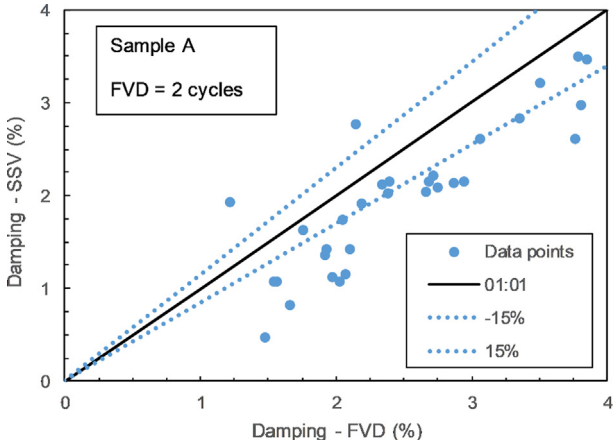

Fig. 7. Comparison of damping between SSV and FVD (at 2 cycles) obtained at small strains for sample A.

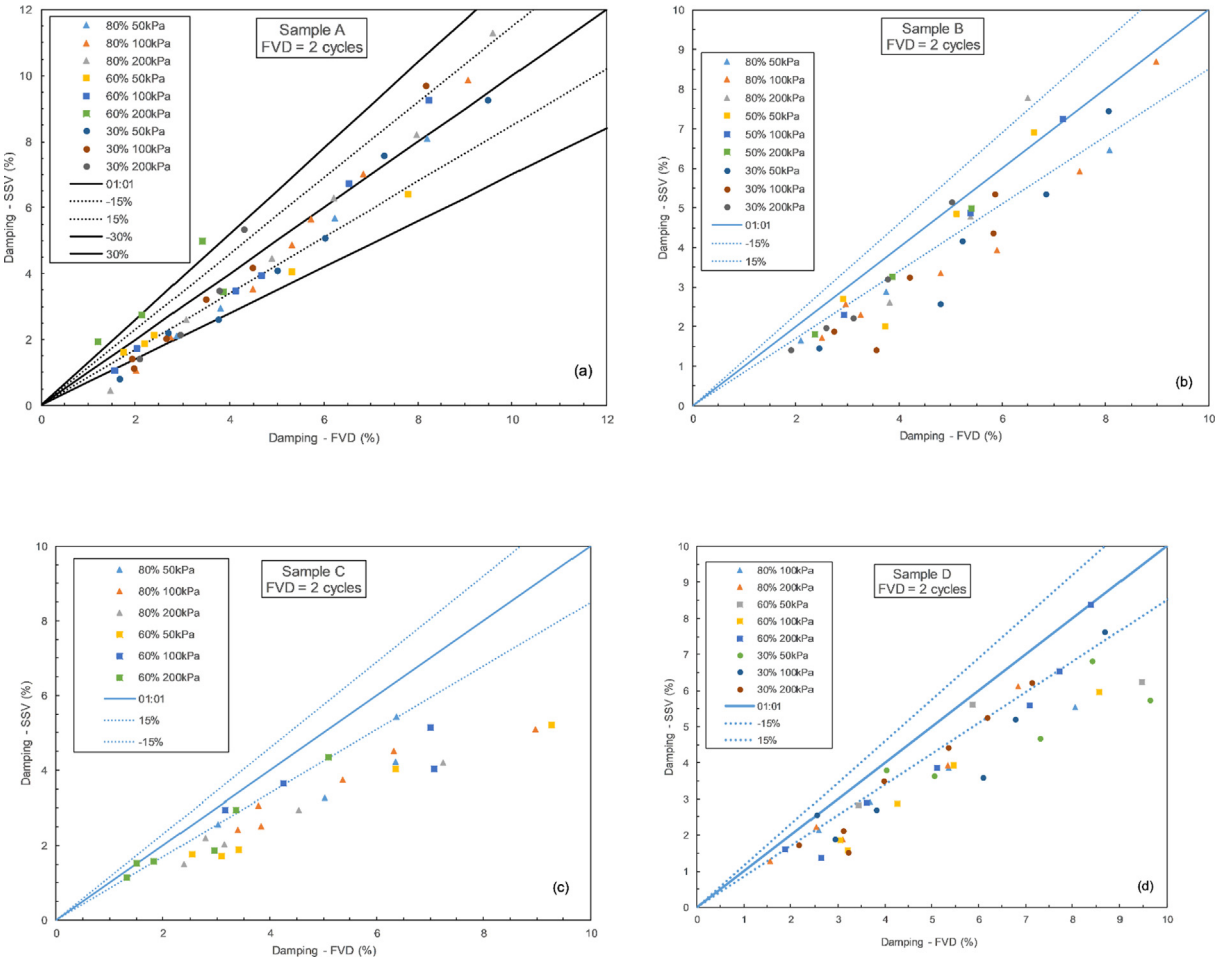

Fig. 8. Comparison of damping between SSV and FVD obtained at small to medium strains (a) for sample A (SP-poorly graded sand), (b) for sample B (SM-silty sand), (c) for sample C (CL- clay of low plasticity), (d) for sample D (CL- clay of low plasticity).

bandwidth method is considered suitable for the very small strain dynamic testing. A similar conclusion was also drawn by Ni (1987), Darendeli (2001), and Khan et al. (2008). Therefore, it is recommended that the SSV (Half-power bandwidth) should be adopted over FVD for the determination of material damping at very small shear strain range. It has also been suggested by Blake (1987) that the half-power bandwidth method should be used for the damping value <10%.

Fig. 8(a)–(d) shows the comparison of the damping ratio between the steady-state and free-vibration method derived at small to medium strain levels. All the data points correspond to samples A, B, C, and D tested at a relative density of 30%, 60%, 80% under the confining pressures of 50, 100, 200 kPa. Fig. 8(a) depicts that most data points at medium strain levels fall within the scatter of ±15% with an exemption of some data points in the SSV and FVD method. This observation accords with the results of Senatakis et al. (2015) for dry sand. This result indicates that the difference in the damping ratio between the two methods at medium strain levels is insignificant for the chosen sand (sample A). However, this does not appear to be the case for samples B (SM), C (CL), and D (CL), as shown in Fig. 8(b)–(d). It was found that in the case of samples B, C, and D, the scatter range between the two methods exceeds ±15%. It mostly falls within ±30% of the data points, even if some data points are discarded. At present, it is unclear if soil type makes the difference wider between SSV and FVD or due to some other factors. Thus, further study on those lines is encouraged.

For strain amplitude larger than the threshold strain (i.e., at medium strain), the damping ratio calculated from the half-power bandwidth method is questionable due to the non-symmetry and non-linearity of the frequency response curve. However, the damping ratio calculated from the free vibration decay (FVD) does not depend on the non-symmetrical response of the frequency response curve. It depends on the number of cycles selected to calculate the damping ratio (as previously discussed). Therefore, when soil response is non-linear at mid strain level (>0.005%), the use of the FVD method is recommended to calculate the damping ratio (at 2nd or 3rd successive cycles). It is because of its best possible fit and less ambient noise associated with a smaller number of cycles. Choosing of damping value from the free-vibration decay method at small strain levels should be avoided, while the resonant column test is carried out on soil samples. On the other hand, the SSV method is recommended to use at the lower

amplitude of vibrations (<0.005%). The results of this study further support that previously published damping data (in the literature) which were obtained without considering the caveats of these two methods and did not account for the apparatus damping, should be reassessed; and careful consideration is recommended before using it for any geotechnical analysis.

5. Effect of confining pressure and relative density on damping ratio

The influence of confining pressures and relative density on the damping ratio obtained from the SSV and FVD methods is investigated for four soil types (samples A, B, C, and D) and discussed in this section. The samples were prepared at three different states as loose (30%), medium (60%), dense (80%), and the resonant column test was performed at three different confining pressures (50, 100, 200 kPa). The representative results obtained from several test series illustrating these effects are presented in Fig. 9 (a)–(f). The influence of soil type on the damping ratio results is presented in Fig. 10. Note that the threshold strain selected between the SSV and FVD method is 0.005%, as above this threshold frequency response curve becomes unsymmetric in SSV and below this threshold ambient noise contributes (in FVD). Thus, to plot Figs. 9 and 10, the SSV method is adopted in small strain damping measurement (<0.005%), and the FVD method (2 successive cycles) is adopted in medium strain damping measurement (>0.005%).

The effect of confining pressure on the variation of damping ratio for coarse-grained soil sample (sample A)

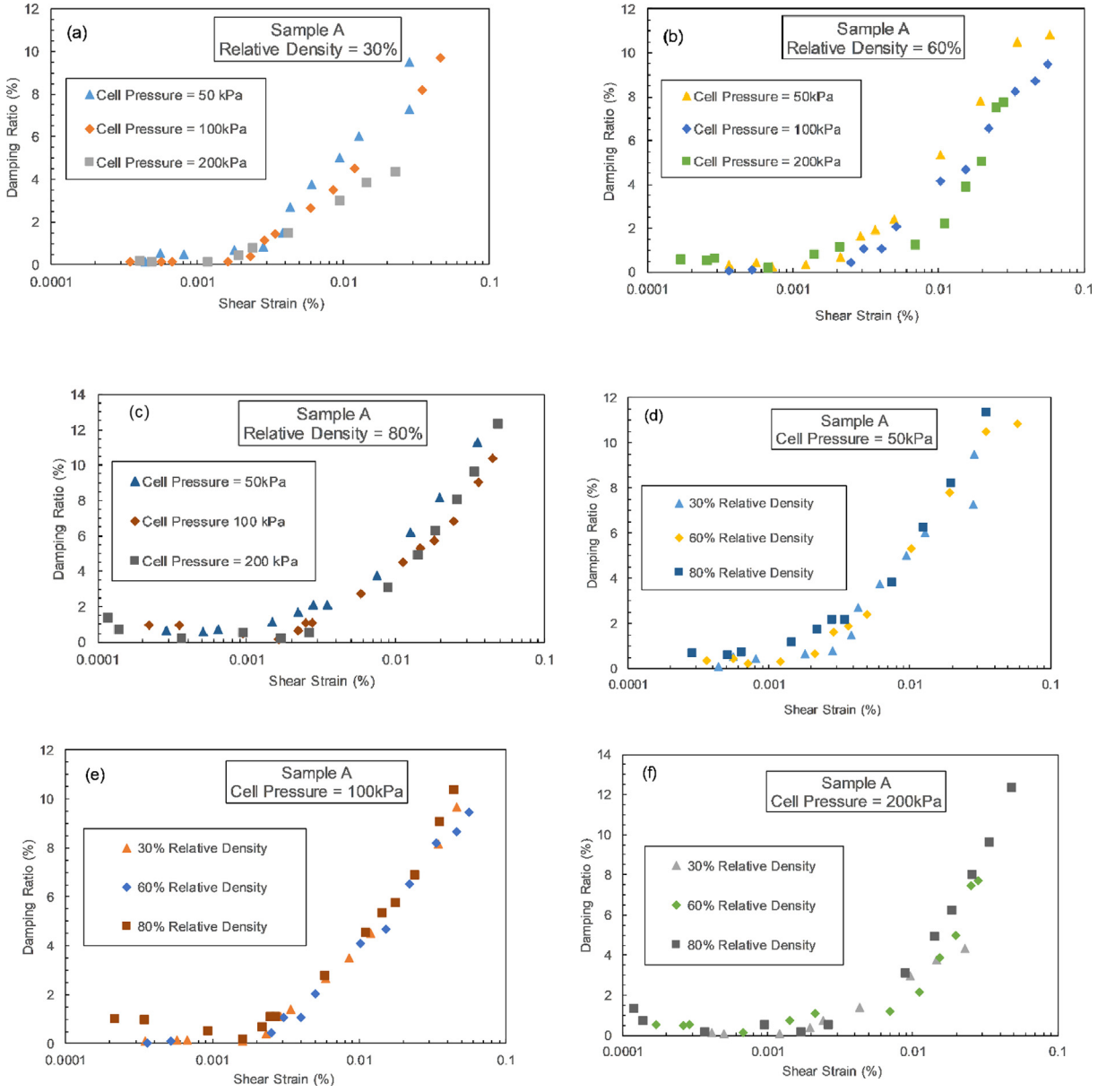

Fig. 9. (a)–(c) and (d)–(f) Variation of damping ratio with respect to confining pressure & relative density at small to medium strain level: Representative Results.

is presented in Fig. 9(a)–(c), and results for the effect of relative density are illustrated in Fig. 9(d)–(f). It can be observed from Fig. 9(a), (b), and (c) that for a given shear strain amplitude (medium strain level), the damping ratio decreases with the increase of the confining pressures. The damping value is maximum for 50 kPa confinement and minimum for 200 kPa confinement at a given relative density. The same trend is also found for other soil samples (samples B, C, and D), which is not shown here to avoid overlapping in the data. For a given specimen density, with the increase in confining pressure, the particle-to-particle contact forces increases, and the void space between them is decreases (due to denser packing). As a result, the wave propagates faster through the medium and decreases the attenuation of waves, decreasing the damping ratio at greater confining pressures (Madhusudhan and Senetakis, 2016). Thus, these results reveal that the influence of confining pressures on the damping properties of the soil is significant at medium strain levels. A similar finding is also reported by Kokusho (1980); Ni (1987); Stokoe et al. (1999); and Mog and Anbazhagan (2018) in the literature. However, at small strain levels (<0.005%), its influence is insignificant (which is also evident from Fig. 9a, b, and c).

It can be observed from Fig. 9(d), (e), and (f) that at a given value of shear strain and confining pressure, the damping ratio increases with the increase of the relative density of the coarse-grained soil. The damping ratio is observed to be maximum for 80% relative density and minimum for 30% relative density specimen, though there is less variation in the value. Also, in most cases, the coinciding value of damping is noticed. The variation in the value of damping tested at three different relative densities is not that significant (<2%). The results concord with the findings of Sitharam et al. (2008), and Mog and Anbazhagan (2018). Likewise, the damping value is observed to be higher for densely packed specimens than the loosely prepared specimen for fine-grained soils (CL). The difference between them is rather small and can be ignored for all practical purposes. Hence, it can be stated that relative density does have a negligible influence on the damping ratio of coarse-grained and fine-grained soil. It can also be seen from those Figs. that damping ratio remains nearly constant or linear up to shear a strain amplitude of 0.001% above which level damping increases with the increase in the shear strain as also explained in the proceeding section.

6. Effect of the type of soil on damping properties

The influence of the soil type on the damping ratio subjected to resonant column testing under three different confining pressures prepared at three different relative densities is presented in Fig. 10 for four types of chosen soil. The variation of damping ratio against the small to medium shear strain range for sand specimens (combined results of sample A and B) is illustrated in Fig. 10(a), while for fine-grained specimens (combined results of sample C and D) is illustrated in Fig. 10(b). It can be observed from Fig. 10(a) that the sand specimen behaves like an elastic body below the shear strain level of 0.001%. That is, the damping ratio is nearly constant, and its value is observed to be <2% in small strain levels (<0.005%). Above the strain level of 0.001% for both sands A and B, the damping value is nearly linearly increasing with the increase in logarithmic strain (in medium strain levels). It was also observed that sample A exhibits a slightly higher value of damping than sample B at a given relative density and confining pressure, though there is little variation. A larger effect of confining stress in sandy soils (sample A) than in silty soils (sample B) is also evident from Fig. 10(a). The reason may be attributed to the variability in the characteristics of the coarseness of the grain size, soil structure, and shapes of the sand material.

Likewise, similar observations were noticed from samples C and D (CL), as shown in Fig. 10(b), except in this case, the slope of the increasing trend of damping ratio is somewhat lower (or flatter) than those of sand specimens. Also, there is hardly any change in the value of observed

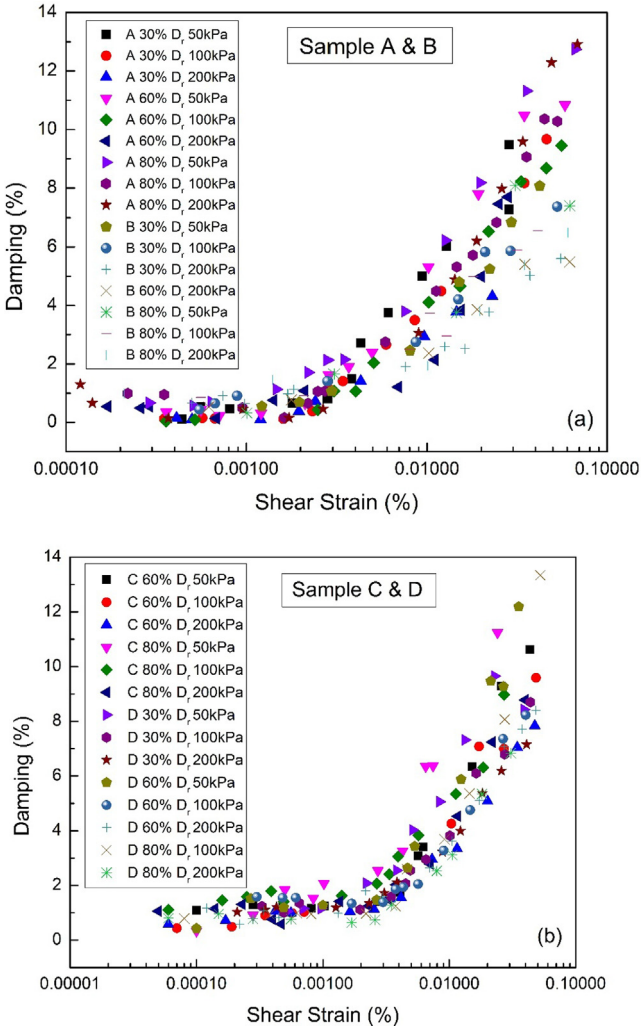

Fig. 10. (a) Damping ratio vs. shear strain amplitude for sample A & B (Sand); (b) damping ratio vs. shear strain amplitude for sample C & D (Clayey silt).

Table 3
Minimum damping ratio obtained for different test samples in the present study.

Test Material	Confining pressures (kPa)	Relative density (30%)	Relative density (60%)	Relative density (80%)
Sample A	50 kPa	0.11	0.23	0.57
Sample A	100 kPa	0.12	0.15	0.16
Sample A	200 kPa	0.1	0.14	0.14
Sample B	50 kPa	1.05	1.2	
Sample B	100 kPa	1	1.05	0.99
Sample B	200 kPa	1.03	0.83	0.77

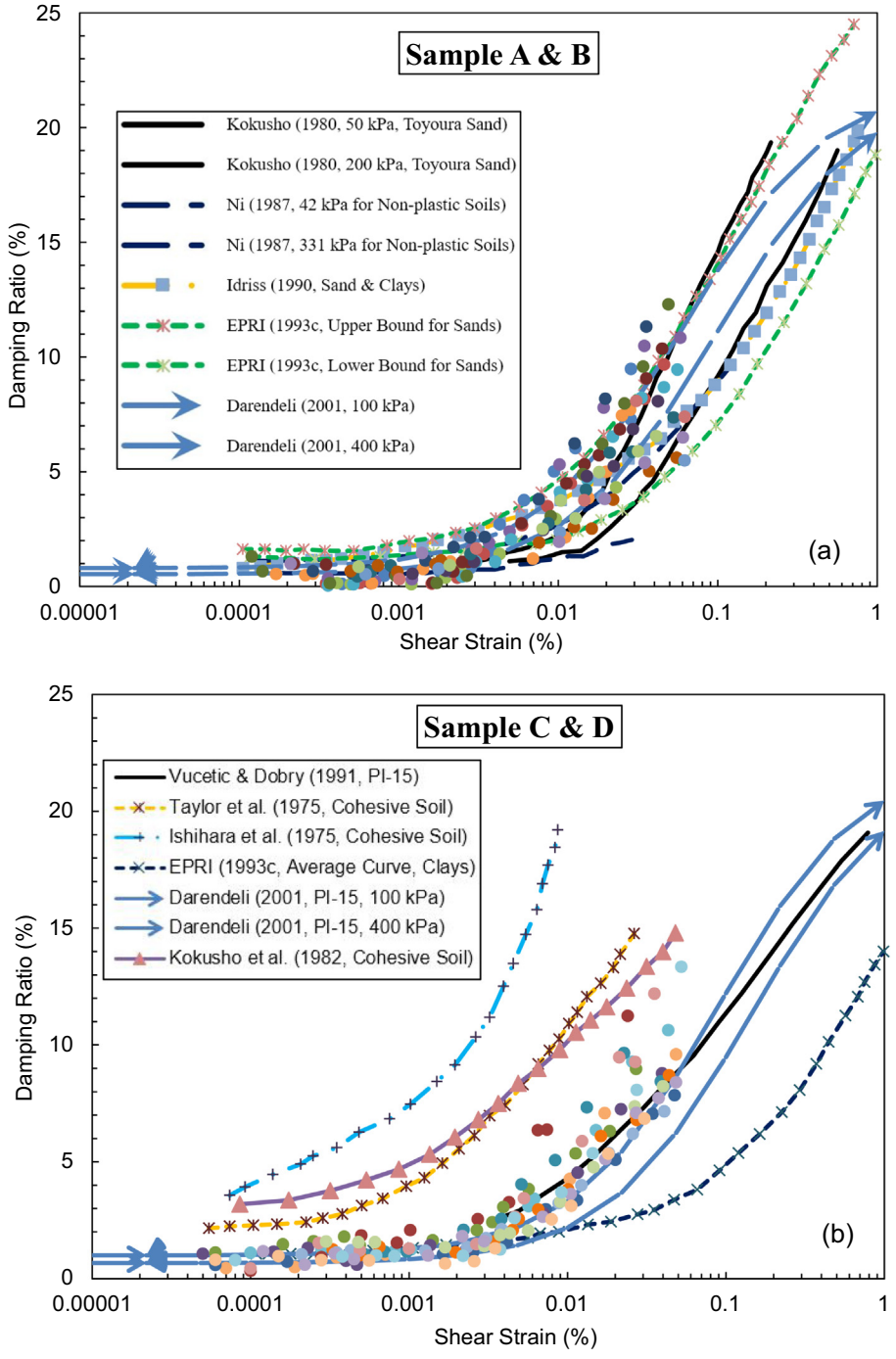

Fig. 11. (a) and (b) Comparison of damping ratio with other investigators for sands and cohesive soils.

damping between samples C and D, as noticed. Mostly, the damping values closely overlap with each other at a given confining stress and relative density. This may be due to nearly the same composition of silt and sand with a slight difference in clay content between these two samples (C and D) as enumerated in Table 1. It was also found that [from Fig. 10(a) and (b)], damping value is observed to be a little higher for clayey silt soils than those of sandy soils. The reason may be attributed to the soil fabric (or arrangement of the soil particles) due to the mixtures of sand, silt, and clay proportions. The initial rates of increase in damping ratio are also higher for clayey silty soils than for sandy soils. This result is in concords with the finding of Hardin and Drnevich (1972). Further, little scatter in the damping data is noticeable above the shear strain level of 0.01% in the case of silty sand samples [Fig. 10(a)], whereas data fall in a narrow band in the case of clayey soils [Fig. 10 (b)].

Also, it was observed that the minimum damping ratio for the sand specimen (sample A), i.e., D_{min} is found to decrease slightly with the increase in the confining pressure, which is consistent with the general trend, and are in line with those of previous studies (Cho et al., 2007; Senetakis et al., 2012; Senetakis and Madhusudhan, 2015; Payan et al., 2016). However, in some cases, no systematic pattern is found with other soil samples (B, C, and D), though little or no variation in D_{min} is observed. Further research is underway considering different types of sands, naturally deposited silts, and clayey soils to put more light on this aspect. The D_{min} as extracted from the resonant column testing for samples A and B is enumerated in Table 3. The minimum damping ratio (D_{min}) of sand and silty sand samples ranges between 0.10 and 0.67%, while for clayey silt soils, it ranges between 0.33 and 1.05%. That is, the D_{min} is little high for clayey silt soils than those of the sandy soils.

7. Comparison of damping ratio with existing curves in the literature

The damping ratio obtained in this research from the resonant column testing (from SSV and FVD) for both sandy soils and clayey silts were compared with the available curves in the literature and presented in Fig. 11. The summary of the test database for the damping ratio curves used in this study for the comparison purpose is listed in Table 4. In Fig. 11(a), the strain dependency damping curves obtained for sample A and sample B, are compared with those obtained by researchers Kokusho (1980); Ni (1987); Idriss (1990); EPRI (1993); and Darendeli (2001) for various kinds of sandy soils. It is noticed that damping values obtained in the present studies are found to be quite different from some of those investigators. The current damping data exhibits a slightly higher value than those of researchers at medium strain levels. It appears that the range of damping ratio does not fit well within the range of those of Kokusho (1980); Ni (1987); and Idriss (1990) curves. However, the sand curves proposed by the EPRI (1993); Darendeli (2001); and Zhang et al. (2005) are observed to be reasonably consistent with the results obtained in the present study for sandy soils. Although, the significant difference lies with D_{min}, which is found to be slightly lower than those investigators. A slight variation in the rates of the increasing trend of damping with respect to shear strain is also noticeable. These variations are believed to be arising due to the certain drawbacks associated with the damping measurement in the old generation equipment in previous studies.

Fig. 11 (b) shows the combined results of C and D samples corresponding to the relative density of 30%, 60%, 80%, and confining pressure of 50, 100, 200 kPa with various kinds of cohesive soil curves (average curves) available in the literature. It is observed that the damping ratio in the present study falls (for the clay of low plasticity) very much on the lower side from those of cohesive soils, as reported by Ishihara et al. (1975), Taylor et al. (1975), and Kokusho et al. (1982); and it falls very much on the upper side from those reported by EPRI (1993). However, the results are in good agreement with the average damping curves as proposed by Vucetic and Dobry (1991) and Darendeli (2001) for clays with a plasticity index of 15. Further, it is interesting to note that the back-calculated damping ratios from in situ data of four vertical array sites (Kokusho et al., 2005), compared with the lab-test data in Fig. 11(a) and (b), revealed that back-calculated damping ratios of one

Table 4
Summary of test conditions of damping curves used for the comparison purpose.

Reference	Test materials	Test type	Strain range (%)	Confining pressures (kPa)
Kokusho (1980)	Clean sands	Cyclic triaxial	0.0005 – 0.56	20 – 300
Kokusho (1982)	Cohesive soil (Primary Consolidation)	Cyclic triaxial	0.0001 – 0.1	45–500
Ni (1987)	Non-plastic soils	RCTS	0.0001 – 0.10	42 – 331
Idriss, 1990	Sand and clays,	–	0.0001 – 1.0	Single curve
EPRI (1993c)	Sands	RCTS	0.0001 – 1.0	Upper bound & lower bound curves
Darendeli (2001)	PI = 0, & PI = 15 (Empirical)	RCTS	0.00001 – 1.0	100 – 400 kPa
EPRI (1993c)	Clays	RCTS	0.0001 – 1.0	Average curve
Ishihara et al. (1975)	Cohesive soils	Cyclic triaxial	0.00001 – 0.01	Average curve
Taylor et al. (1975)	Cohesive soils	Torsional shear	0.00001 – 0.03	Average curve
Vucetic & Dobry (1991)	Non-plastic soils & Clays	Cyclic triaxial	0.003 – 0.30	Single curve
Zhang et al., 2005	Quaternary, Tertiary & Saprolite soils (PI = 0)	RCTS	0.0001 – 1.0	Mean Curve, (100 kPa)

of the sites (KNK) are comparable with the present lab-test data. In both cases, the observed damping ratio is <2% at a small strain regime. Note that the back-calculated damping ratio curve of Kokusho et al. (2005) is not plotted in Fig. 11 to avoid overlapping of the curves.

This investigation suggests that there is a need to develop the dynamic model for Indian soils to capture the correct trend of dynamic curves for a wide strain range. The small strain damping curve as established in the present study should be useful in the site response analysis or any dynamic geotechnical analysis if enough information concerning the soil type or gradation is available, as it is preferable to use an upper and lower range of curves for the complete analysis in order to capture the strain dependency and other essential factors.

8. Summary and conclusions

The small strain dynamic soil properties are particularly important for the analysis in the foundation vibration problems. It provides a fundamental condition for large strain dynamic properties. Hence, it is imperative to estimate the correct damping ratio of the soil material in order to carry out the site response analysis more accurately. Thus, this paper addressed the caveats between two classical approaches (i.e., Steady-State Vibration and Free Vibration Decay methods) of damping estimation in the resonant column testing for a relatively small strain range. The major parameter focused here is the number of cycles in two test methods SSV and FDV, and the appropriate method to be adopted concerning shear strain level. Besides, the effects of relative density, confining pressure, and soil types on the damping ratio were also studied. The following conclusions can be drawn from the present study:

(1) The effect of the number of successive cycles on the damping ratio is significant for all the chosen soil samples at small to medium shear strain amplitudes. The damping ratio adopted from 2nd or 3rd successive cycles is recommended to use at medium strain levels (>0.005%) in FVD, because of its best fit and correlation coefficient.
(2) It was observed that the scatter of the data points between the two methods was more than ±15% for all the chosen soil types except for the sand sample. The difference in damping results between the two methods stems partly due to the contribution of ambient noise at lower strain amplitudes (in FVD) and partly due to the number of applied cycles more than thousands in SSV and only tens in FVD.
(3) Due to non-symmetry and nonlinearity in the frequency response curves in SSV for strain-level exceeding the threshold strain (~0.005%), SSV is rec-

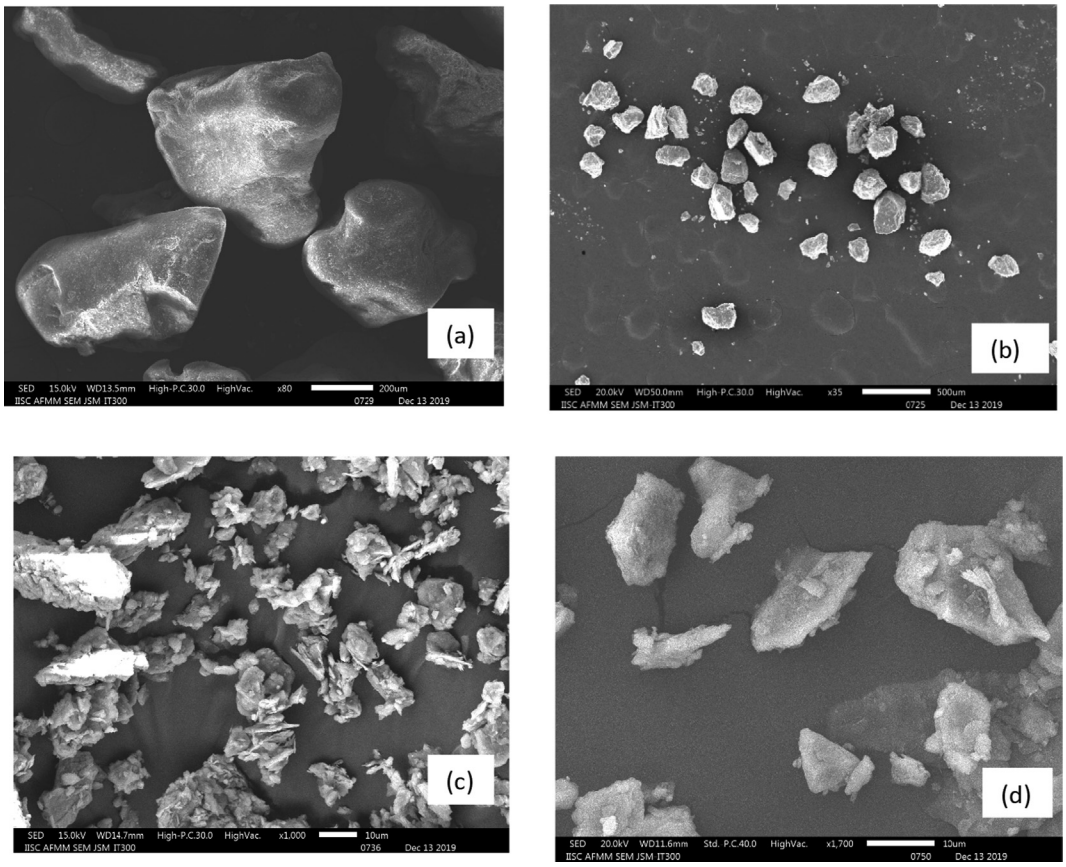

Fig. A1. Scanning electronic microscope images of four soils, (a) Sample A, (b) Sample B, (c) Sample C, and (d) Sample D.

ommended to use for lower amplitude damping measurement. However, since damping determination from FVD does not depend on the non-symmetrical response of the frequency response curve but may get affected by the ambient noise at lower strain amplitudes, the FVD (at 2nd or 3rd successive cycles) is recommended to use for mid-strain damping measurement (>0.005%). The results of this study suggest that the caveats of these two methods should be accounted for while making damping measurements in resonant column testing.

(4) The damping ratio of the tested soils is influenced by the effective confining pressures at medium strain levels. The damping ratio increases with the increase in confining pressures. Nevertheless, at small strain ranges, its influence is insignificant. Similarly, relative density appears to have a negligible effect on the damping value for all the tested soil samples.
(5) It is noticed that clayey silt soils (samples C and D) tend to exhibit a little higher damping value than for sandy soils (samples A and B). The minimum damping ratio, D_{min} observed to increase slightly with

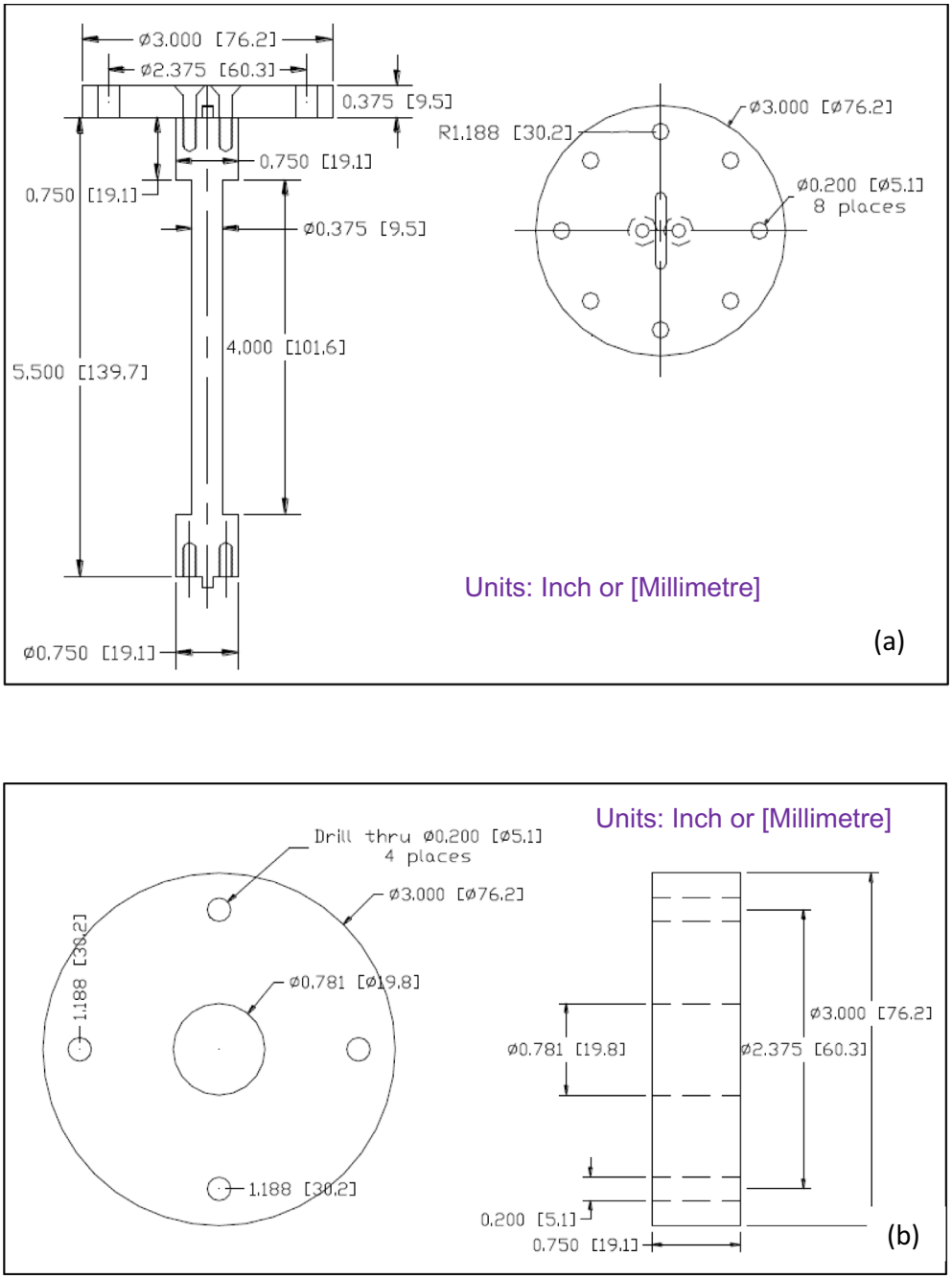

Fig. A2. (a) Calibration specimen geometry, and (b) added mass geometry (specimen top cap). All the units are provided in inches and millimetres together; the values in square brackets indicate the alternate units in mm.

the increase in confining pressures for sand sample (sample A), though its pattern is unsystematic (in some cases) for other tested soils. The D_{min} is found to be a little higher for clayey silt soils (ranges between 0.33 and 1.05%) than those of the sandy soils (ranges between 0.10 and 0.67%).

(6) The damping curves obtained for sands (samples A and B) as compared with other investigators revealed that the damping data presented in this study exhibit a little higher value than those of investigators at medium strain levels. Also, the D_{min} value is observed to be slightly lower than those of investigators.

(7) Similarly, combined damping results of C and D (clayey silt soils) tend to fall much lower side than the curves proposed by previous investigators for cohesive soils and much on the upper side from EPRI (1993c) proposed curves. The damping ratio curves developed in the present study should be useful in the site response analysis or any dynamic geotechnical analysis if enough information concerning the soil type or gradation is available.

Acknowledgments

Authors thank "Board of Research in Nuclear Sciences (BRNS)," Department of Atomic Energy (DAE), Government of India for funding the project titled "Probabilistic seismic hazard analysis of Vizag and Tarapur considering regional uncertainties" (Ref No. Sanction No 36 (2)/14/16/2016-BRNS).

Appendix. *Section 1*

Damping ratio determination for prescribed cycles from the free vibration decay (FVD) data

After the resonant column test is completed, GCTS software calculates the damping ratio using the free vibration data as shown in Fig. 2 (in the manuscript) and using the "peak and valley sensitivity for damping data" value. The peak and valley sensitivity for damping data sets the sensitivity limit (threshold) for peak and valleys of the free vibration data. Its unit is the same as that of the unit of strain. By changing the values of peak and sensitivity in the GCTS resonant column software, the damping ratio is calculated for the various number of cycles as described below.

Fig. A3 displays a typical window of how the damping ratio is determined for the data shown in Fig. 2 (in the manuscript). It can be observed that for a selected (input) value of 0.002% peak and valley sensitivity, only 2 cycles are greater than this peak and valley sensitivity; thus, only two points were used in the damping ratio determination. A least square criterion is used to determine the slope of the line for the plot of strain amplitude versus cycles. In this case, since we have only 2 points, the R^2 (i.e., coefficient of determination) value is 1, indicating that the line goes through both points. However, from the free vibration data (in Fig. A3) itself, one can see more cycles can be used for damping ratio determination.

To generate more cycles, the peak and valley sensitivity is decreased to a value of 0.0001%, meaning more cycles will meet or exceed the sensitivity value; thus, there will

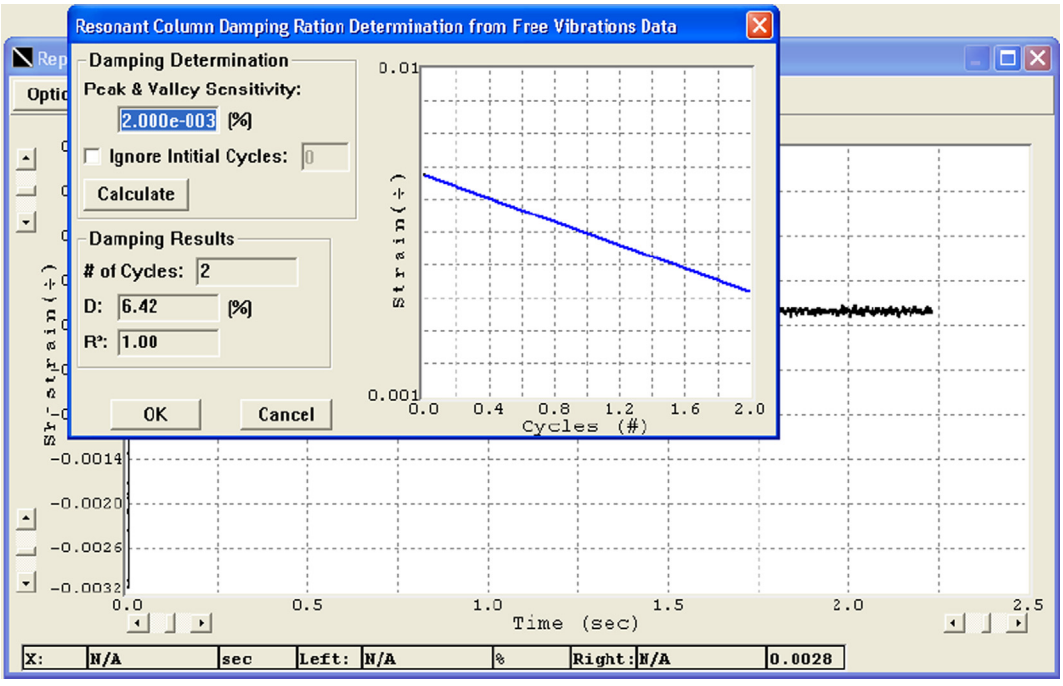

Fig. A3. Damping determination windows from free vibration data for first selected peak and valley sensitivity.

be more cycles in the damping ratio calculation. The recalculated damping results is displayed in Fig. A4.

However, at this stage, there are now 44 cycles in the calculation, but the R^2 has become 0.55; this means the data is no longer linear, which can be verified by simply looking at the plot. From the plot, it appears that the cycles data is only linear to cycle 10.

So now, a value of 0.00035% is selected for the peak and valley sensitivity, and the calculated damping ratio is shown in Fig. A5. As can be seen, now there are only 10 data points in the damping ratio calculation, but the R^2 has become even worse at 0.24, meaning the data is not linear at all.

However, from visual inspection of Fig. A5, one can see that data is linear with the exception of the first cycle point. Therefore, the first cycle point is removed from the damping ratio calculation, and the final calculated damping ratio window is displayed in Fig. A6. As can be seen, the R^2 has become 1, meaning that the cycles data is very linear; thus, the user can be confident that the determined damping ratio is a good estimate. Now, the damping ratio is 4.62% at 9 cycles, whereas firstly the damping ratio was 6.42% at 2 cycles.

In the present study, the above procedure is followed to calculate the damping ratio for all the tested soils specimens and for prescribed cycles. The calculation of the

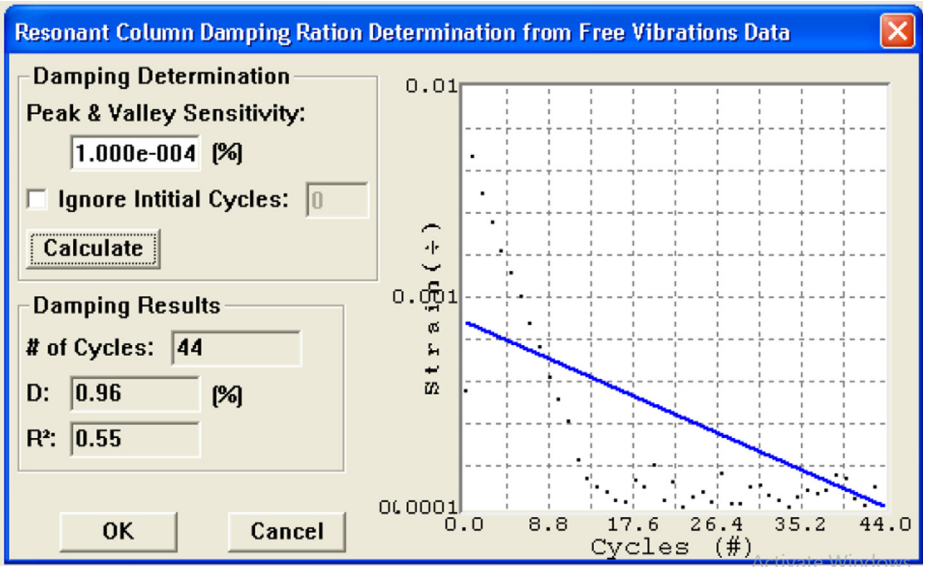

Fig. A4. Damping determination by selecting small peak & valley sensitivity.

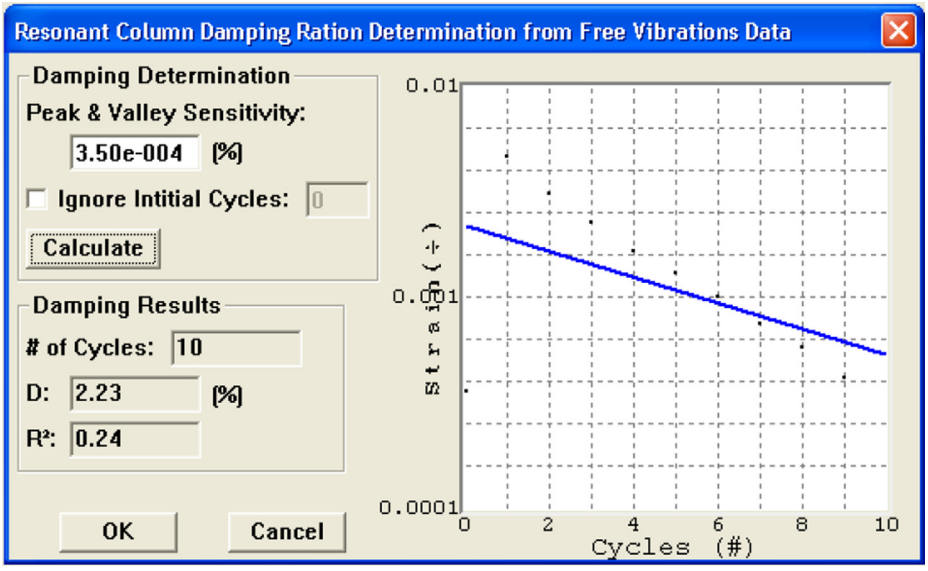

Fig. A5. Damping determination by selecting a good peak & valley sensitivity value.

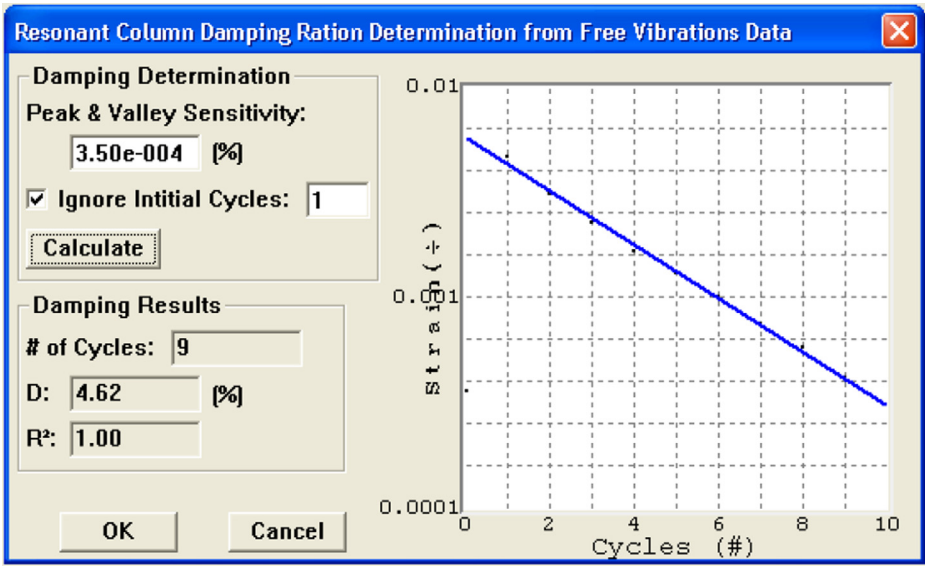

Fig. A6. Damping determination by selecting a final peak & valley sensitivity value that yields the good calculation parameters.

damping ratio using the above procedure by changing the peak and valley sensitivity value is a bit laborious and time-consuming process, as the selection of the peak and valley sensitivity value involves several iterative processes.

References

ASTM Committee D-18 on Soil and Rock, 2017. Standard Practice for Classification of Soils for Engineering Purposes (Unified Soil Classification System) 1. ASTM International.

ASTM. D4015, 1992. Standard test methods for modulus and damping of soils by resonant-column method. Annual Book of ASTM Standards. USA: ASTM International.

Blake, R.E., 1987. Basic vibration theory. Harris' Shock and Vibration Handbook, S, 2-1.

Bolton, M.D., Wilson, J.M.R., 1990. Soil Stiffness and Damping. Cambridge University Engineering Department.

Darendeli, M. B., 2001. Development of a New Family of Normalized Modulus Reduction and Material Damping Curves. Ph. D. dissertation, University of Texas at Austin.

Drnevich ,VP.,. Ashlock, J.C.., 2017. Measurement of Damping in Soils by the Resonant Column Test. In: Geotechnical Frontiers, pp. 80–91.

Electric Power Research Institute (EPRI), 1993. Guidelines for determining design basis ground motions. Method and guidelines for estimating earthquake ground motion in eastern North America, 1, TR-102293.

GCTS-CATS, 2007. Cyclic Triaxial Test. User's Guide and Ref 2.0:1-195.

Cho, G.C., Dodds, J., Santamarina, J.C., 2007. Closure to "Particle Shape Effects on Packing Density, Stiffness, and Strength: Natural and Crushed Sands" by Gye-Chun Cho, Jake Dodds, and J. Carlos Santamarina. Journal of geotechnical and geoenvironmental engineering, 133 (11), 1474.

Hardin, B.O., Drnevich, V.P., 1972. Shear modulus and damping in soils: measurement and parameter effects. J. Soil Mech. Found. Div.

Idriss, I.M., 1990. Response of soft soil sites during earthquakes. InProc. HB Seed Memorial Symp. 2, 273–289.

Ishihara, K., Nei, M., Ueda, S., Takehara, U., 1975. Response analysis of a reclaimed deposit during earthquakes. In: Proc. 4th JEES, Tokyo, 423:430.

Ishihara, K., 1996. Soil Behaviour in Earthquake Geotechnics. Oxford Science Publications.

Khan, Z.H., Cascante, G., El Naggar, M.H., Lai, C.G., 2008. Measurement of frequency-dependent dynamic properties of soils using the resonant-column device. J. Geotech. Geoenviron. Eng. 134 (9), 1319–1326.

Kokusho, T., Aoyagi, T., Wakunami, A., 2005. In situ soil-specific nonlinear properties back-calculated from vertical array records during 1995 Kobe Earthquake. J. Geotech. Geoenviron. Eng. 131 (12), 1509–1521.

Kokusho, T., 1980. Cyclic triaxial test of dynamic soil properties for wide strain range. Soils Found. 20 (2), 45–60.

Kokusho, T., Yoshida, Y., Esashi, Y., 1982. Dynamic properties of soft clay for wide strain range. Soils Found. 22 (4), 1–18.

Madhusudhan, B.N., Senetakis, K., 2016. Evaluating use of resonant column in flexural mode for dynamic characterization of Bangalore sand. Soils and Foundations 56 (3), 574–580.

Meng, J., 2003. The Influence of Loading Frequency on Dynamic Soil Properties PhD dissertation. Georgia Institute of Technology.

Mog, K., Anbazhagan, P., 2018. Dynamic properties of surface liquefied site silty-sand of Tripura, India. InInternational Congress and Exhibition" Sustainable Civil Infrastructures: Innovative Infrastructure Geotechnology". Springer, Cham, pp. 140–154.

Ni, S.H., 1987. Dynamic Properties of Sand Under True Triaxial Stress States from Resonant Column/torsional Shear Tests. Ph. D dissertation, The University of Texas at Austin.

Papagiannopoulos, G.A., Hatzigeorgiou, G.D., 2011. On the use of the half-power bandwidth method to estimate damping in building structures. Soil Dyn. Earthquake Eng. 31 (7), 1075–1079.

Payan, M., Senetakis, K., Khoshghalb, A., Khalili, N., 2016. Influence of particle shape on small-strain damping ratio of dry sands. Géotechnique 66 (7), 610–616.

Santamarina, C., Cascante, G., 1998. Effect of surface roughness on wave propagation parameters. Geotechnique 48 (1), 129–136.

Senetakis, K., Anastasiadis, A., Pitilakis, K., 2015. A comparison of material damping measurements in resonant column using the steady-state and free-vibration decay methods. Soil Dyn. Earthquake Eng. 74, 10–13.

Senetakis, K., Madhusudhan, B.N., 2015. Dynamics of potential fill–backfill material at very small strains. Soils Found. 55 (5), 1196–1210.

Senetakis, K., Anastasiadis, A., Pitilakis, K., 2012. The small-strain shear modulus and damping ratio of quartz and volcanic sands. Geotech. Test. J. 35 (6), 964–980.

Sitharam, T.G., Ravishankar, B.V., Vinod, J.S., 2008. Dynamic properties of dry sands. Indian Geotech 38 (3), 334–344.

Standard, A.S.T.M., 2000. Standard Test Methods for Liquid Limit, Plastic Limit, and Plasticity Index of Soils. ASTM International, West Conshohocken, PA.

Stokoe, K.H., Darendeli, M.B., Andrus, R.D., Brown, L.T.., 1999. Dynamic soil properties: laboratory, field and correlation studies. In: Proceednings of the 2nd International Conference on Earthquake Geotechnical Engineering 1999, AA Balkema, pp. 811–845.

Vucetic, M., Dobry, R., 1991. Effect of soil plasticity on cyclic response. J. Geotech. Eng. 117 (1), 89–107.

Wang, J.-T., Jin, F., Zhang, C.-H., 2012. Estimation error of the half-power bandwidth method in identifying damping for multi-DOF systems. Soil Dyn. Earthquake Eng. 39, 138–142.

Yamamizu, F., Goto, N., Ohta, Y., Takahashi, H., 1983. Attenuation of shear waves in deep soil deposits as revealed by down-hole measurements in the 2, 300 meter-borehole of the Shimohsa observatory, Japan. J. Phys. Earth 31 (2), 139–157.

Zhang, J., Andrus, R.D., Juang, C.H., 2005. Normalized shear modulus and material damping ratio relationships. J. Geotech. Geoenviron. Eng. 131 (4), 453–464.